ADVANCED MATERIALS

Supporting Information

for *Adv. Mater.,* DOI: 10.1002/adma.202007473

Spatial Control of Probiotic Bacteria in the Gastrointestinal Tract Assisted by Magnetic Particles

*Marjorie T. Buss, Pradeep Ramesh, Max Atticus English, Audrey Lee-Gosselin, and Mikhail G. Shapiro**

Supporting Information

Spatial Control of Probiotic Bacteria in the Gastrointestinal Tract Assisted by Magnetic Particles

Marjorie T Buss[+], Pradeep Ramesh[+], Max Atticus English, Audrey Lee-Gosselin, Mikhail G Shapiro*

[+] These authors contributed equally to this work.

* Correspondance: mikhail@caltech.edu

Supporting Methods

X-ray CT imaging: CT images of the abdominal area (45 x 45 mm field-of-view) were acquired using 3D micro-CT (Rigaku) with a resolution of 90 μm, tube potential peaks of 90 kV, tube current of 88 μA, and imaging duration of approximately 5 min. Mice were sedated during imaging using isoflurane (1%) at various time points after gavage. The magnets/non-magnetic washers were removed prior to imaging and immediately re-attached afterwards. Thresholding and 3D image reconstruction was performed using ImageJ.

MRI: Shortly after dissection, mouse intestines were fixed using 10% formalin at room temperature for 20 minutes. Fixed intestines were washed using cold PBS + 0.1 mM L-ascorbic acid and stored at 4°C until imaging. Before imaging, intestines were cast in a 1% (w/v) agarose gel phantom to minimize susceptibility artifacts. A Bruker 7 T small-animal scanner was used for all MR imaging, with a Rat volume coil (70 mm inner diameter) supplying the RF for ^{1}H spin-excitation and subsequent readout. Given the high relaxivity of the micromagnets gavaged, a 3D UTE sequence (T_E = 20 μs, T_R = 8 ms, N_{avg} = 2) was used to localize micromagnets within the intestines, using an isotropic voxel size of 234 μm. A 3D FLASH sequence, with an isotropic voxel size of 325 μm, was used to obtain anatomical images of the *ex vivo* GI tract specimens.

Scaling estimations: To estimate the approximate sizes of the external wearable magnet and internal micromagnets needed to use CLAMP in larger animals such as humans, we first approximate the wearable magnets as a sphere. This approximation yields an order-of-magnitude scaling insight into the relevant sizes of the magnets used for CLAMP, as well as the expected field and field-gradient strengths. Furthermore, we neglect any azimuthal components, focusing to model just the axial magnetic field for simplicity (Equation 2)[1]:

$$B(z) = \frac{2\mu_0 M R_{\text{magnet}}^3}{3z^3} \tag{2}$$

Here, z is the axial distance from the center of the spherical magnet, M is the volume magnetization, R_{magnet} is the magnet's radius, and μ_0 is the permeability of free space constant. The magnitude of the magnetic field gradient is then given by equation 3:

$$\left|\frac{dB}{dz}\right| = \frac{2\mu_0 M R_{\text{magnet}}^3}{z^4} \tag{3}$$

Substituting these expressions into equation 1 (see main text), the magnitude of the force on the micromagnets is approximated by equation 4:

$$\left|F_{\text{mag}}\right| = \frac{16\pi}{9} \frac{\mu_0 M^2 \Delta\chi R_{\text{bead}}^3 R_{\text{magnet}}^6}{z^7} \quad (4)$$

Where R_{bead} is the radius of the micromagnets and $\Delta\chi$ is the difference in magnetic susceptibility between the micromagnets and the surrounding medium. In mice, the small intestine is at an average distance of 10 mm from the abdominal surface; in humans the small intestine is at an typical distance of 60 mm[2,3]. From our in vivo results, we can conclude that the magnetic forces achieved by CLAMP are sufficient to arrest downstream peristaltic transport of the composite biomagnetic material once formed at a desired GI locus. Similar magnetic forces need to be achieved in larger animals to obtain similar retention of magnetized cells and particles. If we assume that the same magnetic materials are used in larger animals, then M and $\Delta\chi$ are the same, and the following relation must hold:

$$\frac{R_{\text{bead, mouse}}^3 R_{\text{magnet, mouse}}^6}{(R_{\text{magnet, mouse}} + 10)^7} = \frac{R_{\text{bead, human}}^3 R_{\text{magnet, human}}^6}{(R_{\text{magnet, human}} + 60)^7} \quad (5)$$

Here we specifically provide the scaling relationship for use of CLAMP in humans, but the approach is generalizable to any other animal. In our in vivo experiments with mice, the micromagnets had an average diameter of 1.5 μm, so $R_{\text{bead, mouse}} = 7.5 \times 10^{-4}$ mm; and the volume of the wearable magnet array was 1.54 cm^3 , so the equivalent radius is $R_{\text{magnet, mouse}} = 7.16$ mm. To estimate the radius of micromagnets and the permanent magnet needed for use in humans, these values were plugged into equation 5 and $R_{\text{bead, human}}$ was solved for using varying values of $R_{\text{magnet, human}}$ in MATLAB (Figure S7).

Supporting References

[1] J. M. Camacho, V. Sosa, *Rev. Mex. Fis. E* **2013**.

[2] "Small bowel mri (enterography) planning and preparation | mri enteroclysis protocols and indications," can be found under https://mrimaster.com/PLAN SMALL BOWEL.html, **n.d.** Accessed January 2021.

[3] "abdomen anatomy | MRI abdomen axial anatomy | free cross sectional anatomy |," can be found under https://mrimaster.com/anatomy abdomen axial.html, **n.d.** Accessed January 2021.

Supporting Figures

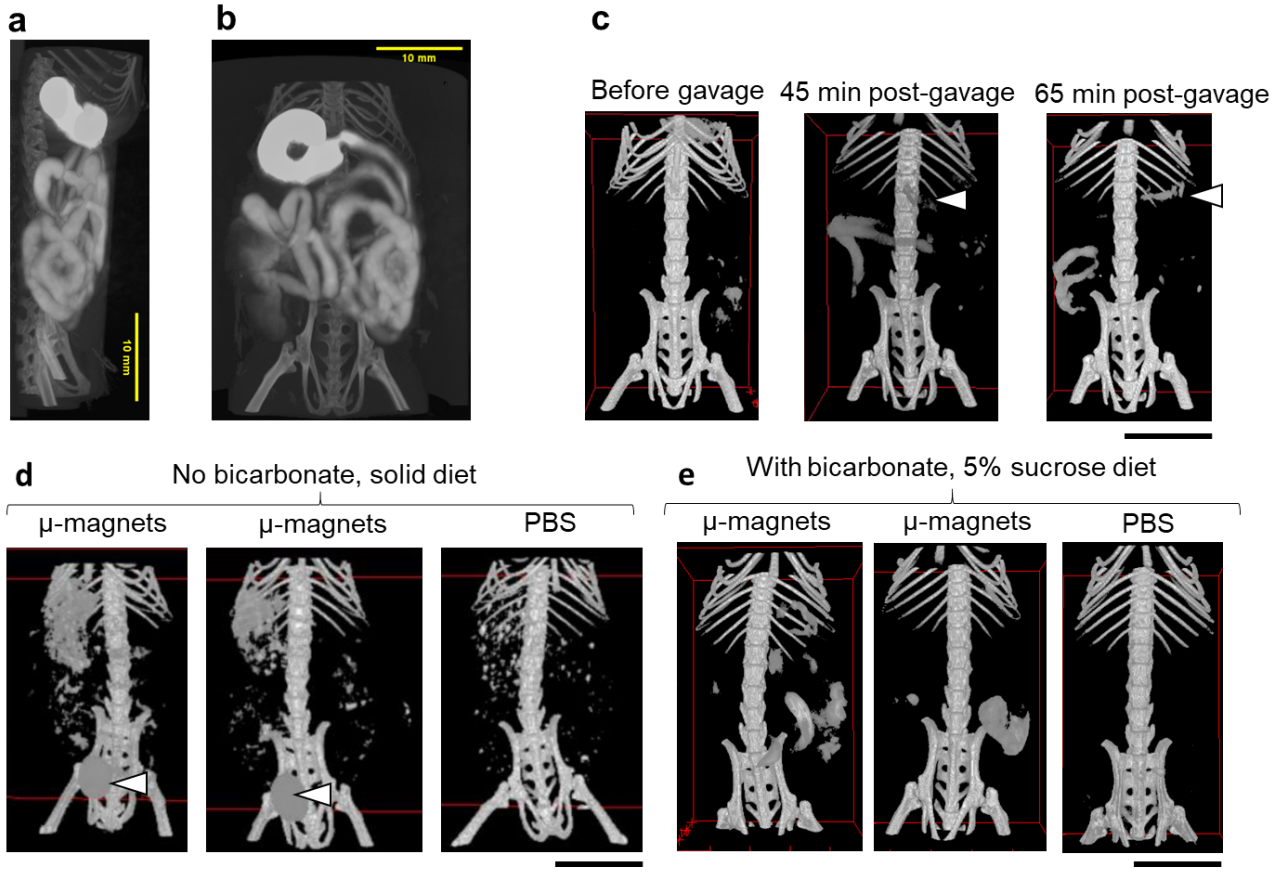

Figure S1. X-ray CT data. a,**b**, Representative sagittal (**a**) and coronal (**b**) X-ray CT images of the mouse GI tract after oral gavage of a CT contrast agent (Isovue-370). **c**, Representative images before gavage, 45-min post-gavage, and 65 min post-gavage of a mixture of micromagnets. The mouse was fasted prior to gavage and given only sucrose water after gavage. The white arrows point to the micromagnets remaining in the stomach. **d**,**e**, Representative images of mice at 6 hours after gavage of micromagnets without bicarbonate (**d**) and with bicarbonate (**e**). Mice in (**d**) were given normal solid food after gavage while mice in (**e**) were given sucrose water after gavage; both were fasted prior to gavage. Arrows in (**d**) point to the signal from iron accumulation in the bladder; no signal from the bladder was observed in (**e**). All scale bars are 10 mm.

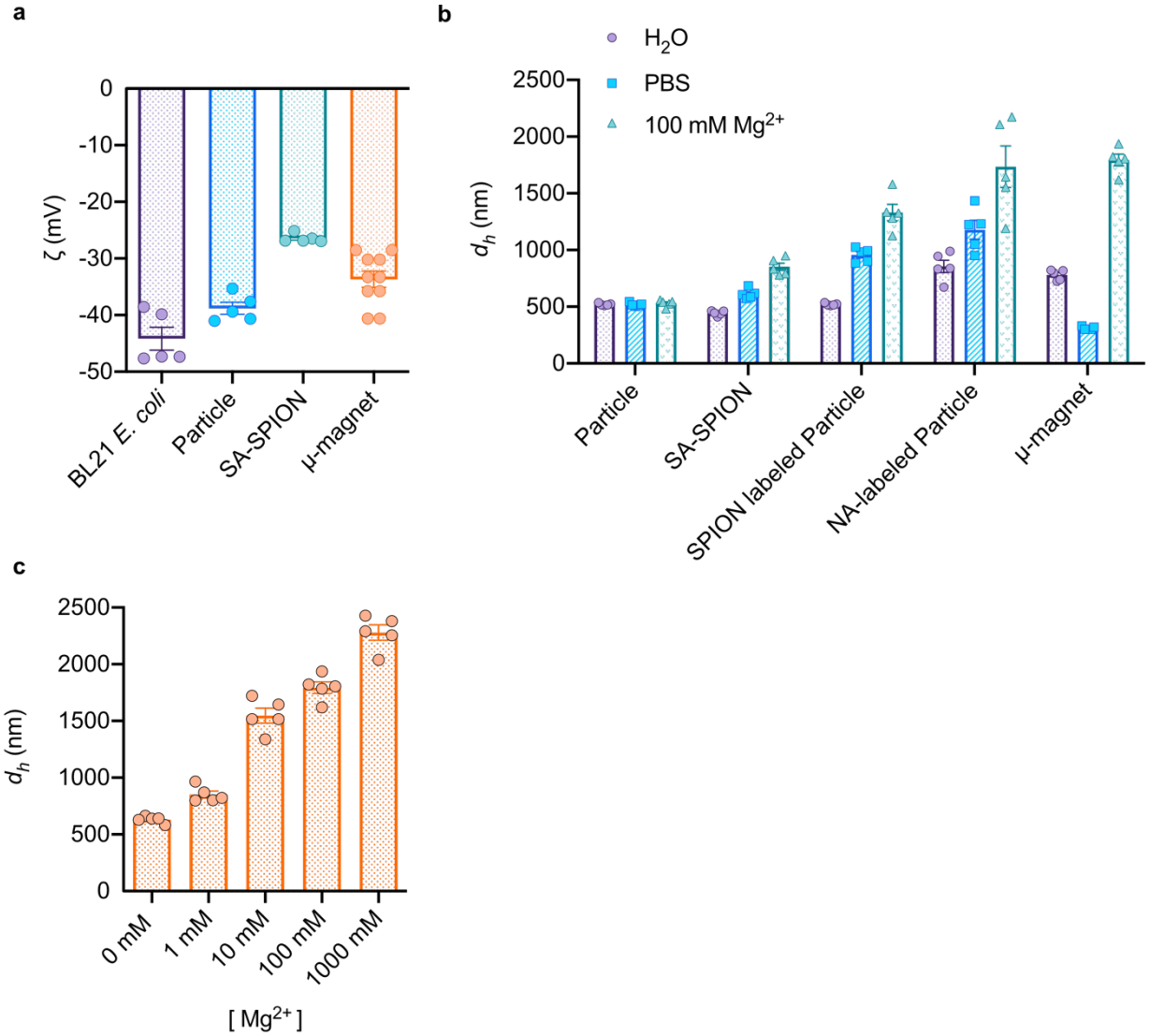

Figure S2. Characterization of particles and cells. **a**, Zeta potential measurements of BL21(DE3) *E. coli*, 0.5 μm fluorescent polystyrene particles, magnetic label (150 nm streptavidin-coated superparamagnetic iron oxide nanoparticles, SA-SPION), and micromagnets (BioMag Carboxyl) used in this study. **b**, Hydrodynamic radius measured by DLS of 0.5 μm fluorescent polystyrene particles, magnetic label (SA-SPION), SPION-labeled particles, Neutravidin (NA)-labeled particles, and micromagnets (BioMag Carboxyl) used in this study in water and 100 mM $MgCl_2$. **c**, Hydrodynamic radius measured by DLS of micromagnets (BioMag Carboxyl) as a function of $MgCl_2$ concentration.

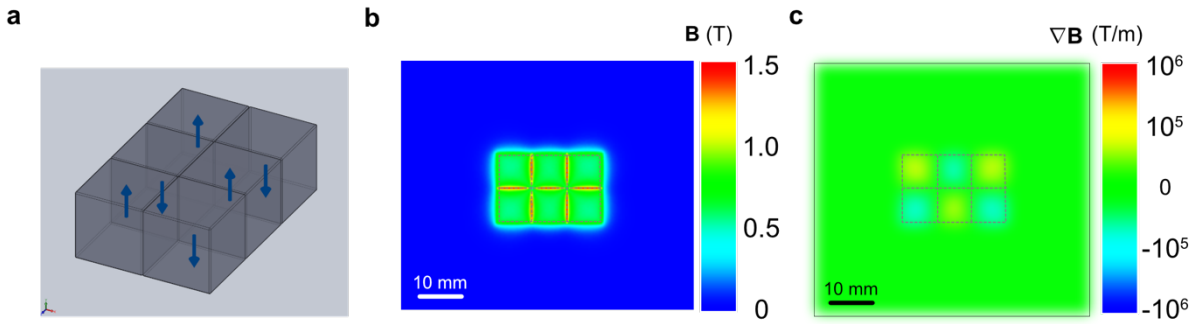

Figure S3. Additional simulation results for the magnet array. a, Schematic of magnet array of 3 x 2 B444-N52 magnets used in in vivo experiments. The magnets were arranged in a checkerboard pattern of alternating magnetization to maximize areas of high field and field gradient strength. **b**,**c**, Simulation of the magnetic flux density (**b**) and magnetic field gradient (**c**) at the surface of the magnet array.

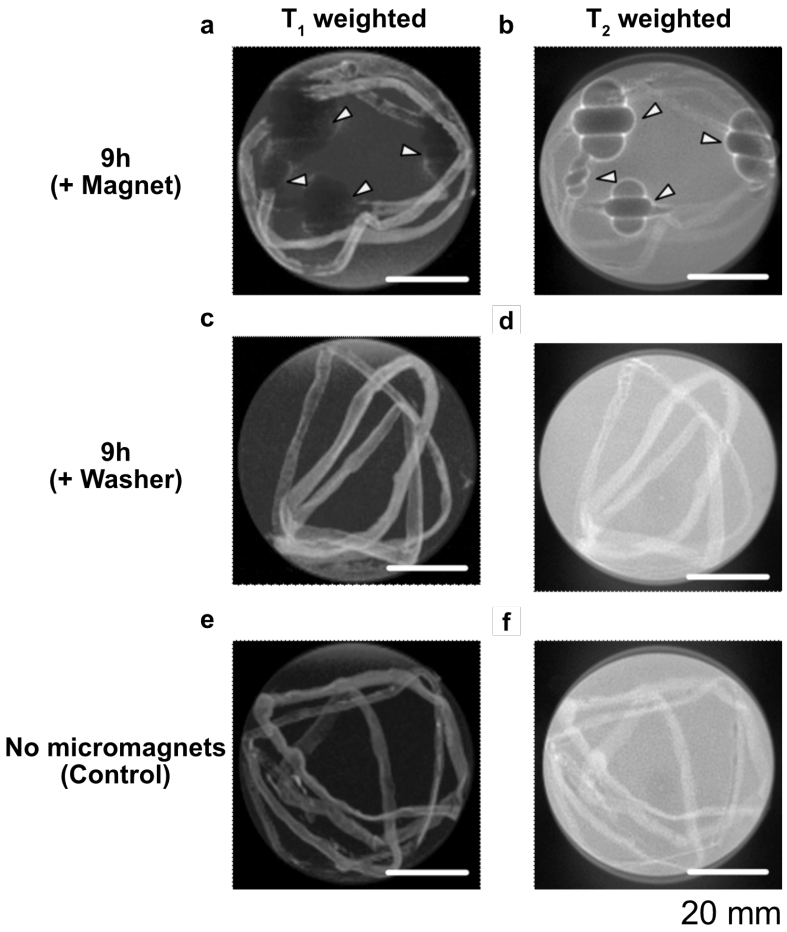

Figure S4. **Representative *ex vivo* MRI on mouse small intestines**. **a**, T1 weighted anatomical image alongside **b**, T2 weighted image of a mouse small intestine (SI), with arrows indicating regions of susceptibility artefacts which are caused by the presence of micromagnets. The SI was isolated from a mouse 9h post-gavage. A magnet was placed on the mouse abdomen 75 mins after gavage with the micromagnet and synthetic-cell mixture. **c**, T1 weighted anatomical image alongside **d**, T2 weighted image of a mouse SI 9h post gavage. A non-magnetic washer of equivalent weight was placed on the mouse abdomen 75 mins after gavage with the same experimental mixture as in (**a**). No susceptibility artefacts were observed in the SI as evidenced by the lack of T2* blooming in the T2 weighted image. **e**, T1 and **f**, T2 weighted images of a control mouse SI respectively. The mouse was not gavaged with any beads but was maintained under the same experimental conditions as in (**a**) and (**c**). The SI was dissected from the GI tract and placed within an agarose matrix to minimize susceptibility artefacts during imaging. All scale bars are 20 mm.

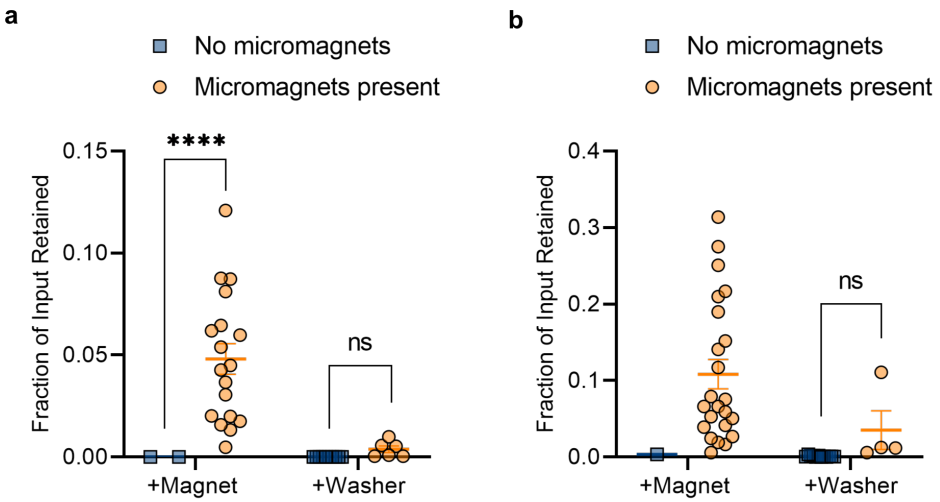

Figure S5. Co-localization of magnetically-labeled *E. coli* and particles with micromagnets in vivo. **a-b**, Fraction of SPION-labeled *E. coli* (**a**) and SPION-labeled particles (**b**) retained in small intestinal segments where micromagnets were observed or absent in a given mouse. Small intestinal segments SI-1 through SI-4 (see Figure 3d-e) were examined by eye for the presence of micromagnets before quantification of the *E. coli* or particles retained. Lines represent the mean and error bars represent the SEM. Asterisks represent statistical significance by the Welch's t test (**** = $p<0.0001$, ns=no significance).

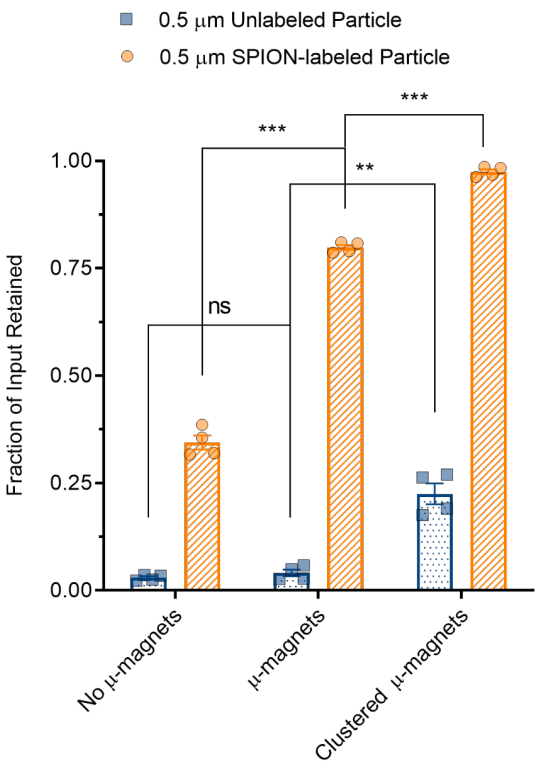

Figure S6. **In vitro efficacy of CLAMP with particles**. In vitro capture of non-magnetic and magnetized 0.5 μm fluorescent particles without micromagnets, with micromagnets, and with clustered micromagnets. The experimental setup is as illustrated in Figure 2 except with particles instead of *E. coli*. Asterisks represent statistical significance by Welch's t test (*** = $p<0.001$, ** = $p<0.01$, ns = no significance).

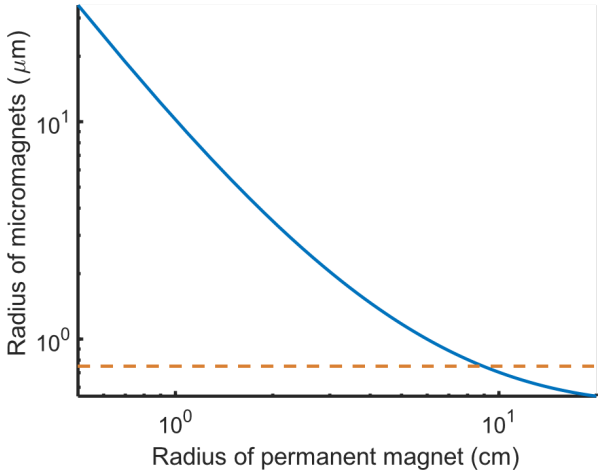

Figure S7. **Estimates for scaling CLAMP to humans**. Radius of internal micromagnets versus equivalent radius of wearable magnet needed to achieve sufficient force to CLAMP cells in the small intestine of humans. The orange dotted line indicates the radius of micromagnets used in our in vivo experiments with mice. Here, we assumed that the wearable magnet is spherical, the small intestine is at a distance of 6 cm from the abdominal skin, and the micromagnets and wearable magnet are made of the same materials as those used in our studies with mice. See supporting methods section for more details.